HHS Public Access

Author manuscript

Anesthesiology. Author manuscript; available in PMC 2018 December 01.

Published in final edited form as:

Anesthesiology. 2017 December ; 127(6): 976–988. doi:10.1097/ALN.0000000000001888.

Anesthesia with dexmedetomidine and low dose isoflurane increases solute transport via the glymphatic pathway in rat brain when compared to high dose isoflurane

Helene Benveniste, M.D., Ph.D.[a], **Hedok Lee, Ph.D.**[a], **Fengfei Ding, M.D., Ph.D.**[b], **Qian Sun, Ph.D.**[b], **Ehab Al-Bizri, M.D.**[c], **Rany Makaryus, M.D.**[c], **Stephen Probst, M.D.**[c], **Maiken Nedergaard, M.D., Ph.D.**[b], **Elliot A. Stein, Ph.D.**[d], and **Hanbing Lu, Ph.D.**[d]

[a]Department of Anesthesiology, Yale School of Medicine, New Haven, CT 06520 USA

[b]Center for Translational Neuromedicine, University of Rochester, NY 14604, USA

[c]Department of Anesthesiology, Stony Brook Medicine, Stony Brook, NY 11794, USA

[d]National Institute on Drug Abuse, Intramural Research Program, Baltimore, MD 21224, USA

Abstract

Background—The glymphatic pathway transports cerebrospinal fluid (CSF) through the brain thereby facilitating waste removal. A unique aspect of this pathway is that its function depends on the brain's state of consciousness and is associated with norepinephrine activity. A current view is that all anesthetics will increase glymphatic transport by inducing unconsciousness. This view implies that the effect of anesthetics on glymphatic transport should be independent of their mechanism of action, as long as they induce unconsciousness. We tested this hypothesis by comparing the supplementary effect of dexmedetomidine, which lowers norepinephrine, to isoflurane only, which does not.

Methods—Female rats were anesthetized with either isoflurane (N=8) or dexmedetomidine + low dose isoflurane, (DEXM-I) (N=8). Physiological parameters were recorded continuously. Glymphatic transport was quantified by contrast-enhanced MRI. CSF, grey and white matter volumes were quantified from T1 maps; and blood vessel diameters were extracted from time-of-flight MR angiograms. Electroencephalograms were recorded in separate groups of rats.

Results—Glymphatic transport, was enhanced by 32% in rats anesthetized with DEXM-I when compared with isoflurane. In the hippocampus, glymphatic clearance was 6-fold more efficient during DEXM-I anesthesia when compared to isoflurane. The respiratory and blood gas status was comparable in rats anesthetized with the two different anesthesia regimens. In the DEXM-I rats, spindle oscillations (9–15 Hz) could be observed; but not in isoflurane anesthetized rats.

Corresponding author: Helene Benveniste, M.D., PhD, Department of Anesthesiology, Yale School of Medicine, 333 Cedar Street, TMP3, Rm. 339, New Haven, CT 06520-8089, Phone: 203-737-1516, helene.benveniste@yale.edu.

Clinical trial and registry URL: Not applicable

Prior Presentations: Not applicable

Conflict of interest: The authors declare no conflict of interest.

Conclusions—We propose that anesthetics affect the glymphatic pathway transport not simply by inducing unconsciousness, but also by additional mechanisms, one of which is the repression of norepinephrine release.

Introduction

The glymphatic pathway is a newly discovered system that clears waste including amyloid-β (Aβ)[1], tau[2] and lactate[3] from the brain. Therefore, a plausible hypothesis has recently emerged, positing that malfunction of the brain's glymphatic waste clearance system may contribute to the pathogenesis of Alzheimer's disease[4]. Anatomically, the glymphatic pathway is defined by the peri-vascular compartment of the cerebral vascular network[1]. The outer perimeter of the peri-vascular space is made up by glial endfeet characterized by high, polarized expression of aquaporin 4 (AQP4) water channels[1]. Studies suggest that the glymphatic pathway removes waste in the following manner: cerebrospinal fluid (CSF) is transported from the subarachnoid space into the brain via the peri-arterial spaces[1]; the AQP4 water channels on the glial endfeet help boost transport of CSF from the peri-vascular compartment into the interstitial fluid (ISF) space[1]. The CSF-ISF exchange process facilitates interstitial waste removal via peri-venous conduits and along cranial nerves[1,5,6] to ultimately drain via lymph vessels located in the meninges[7], head and the neck[8]. The polarized AQP4 expression pattern on glial endfeet is essential for efficient waste clearance[1]. For example, in aging or traumatic brain injury, loss of AQP4 polarization slows down clearance of Aβ and tau[9]; and in post-mortem brain tissue from human afflicted with Alzheimer's disease, the AQP4 expression pattern is inhomogeneous and associated with Aβ plaques[10].

The main controllers of glymphatic waste clearance includes intracranial pressure differentials[11], cardiac pulsation[12] and regulators of ISF space volume[13]. For example, changes in body posture impacts glymphatic transport and Aβ clearance from brain[14]. A most intriguing feature of glymphatic pathway function is its dependency on state of arousal[13], such that glymphatic transport of solutes (including Aβ) accelerates during slow wave sleep or general anesthesia when compared to wakefulness[13]. The underlying mechanism(s) responsible for reduced brain waste removal during wakefulness compared to sleep is not well understood but is associated with central norepinephrine activity since central blockade with alpha adrenergic blockers mimics the effect[13]. Given the association between brain waste removal, norepinephrine activity and state of arousal[3,15], a key question to address would be how anesthetics with different mechanisms of action but with common effects on the state of consciousness influence glymphatic transport patterns? This is important because there may be clinical benefit of enhancing the brain's glymphatic transport during anesthesia/sedation procedures; which could be accomplished if drugs with central norepinephrine lowering effects are used.

Dexmedetomidine is routinely administered to patients in intensive care units and anesthesia settings[16]. Dexmedetomidine is a selective α2 agonist that hyperpolarizes LC neurons, decreasing their firing rate and norepinephrine release[17], thereby inducing a hypnotic effect. Sedation with dexmedetomidine induces a state similar to stage II sleep with an increase in slow-wave activity (0.5–3.5 Hz)[18]. In contrast, inhalational agents such as isoflurane induces

hypnosis, analgesia, amnesia and relaxation by interactions with $GABA_A$, NMDA and glycine receptors[19]. Isoflurane administered at 1.5–2 MAC reduces LC activity but paradoxically increases norepinephrine in the preoptic hypothalamus[20]; and is associated with burst suppression. Given the diverse effects of dexmedetomidine and isoflurane on central norepinephrine, we here test the hypothesis that glymphatic transport will be more efficient during anesthesia that combines dexmedetomidine with low dose isoflurane compared to isoflurane only in the rodent brain. To test this hypothesis we use our previously developed MRI based platform for quantifying glymphatic transport in the rodent brain[21].

Materials and Methods

Animals: The local institutional animal care and use committees at National Institute on Drug Abuse, Intramural Research Program, Baltimore MD, USA, Stony Brook University, Stony Brook, NY, USA and Rochester University, Rochester NY, USA, and Yale University, New Haven, USA approved all animal work. To test our hypothesis, rats were divided into six experimental groups (Table 1). Female Fisher 344 rats (200–300g) were used in groups 1, 2, 5 and 6; and female Sprague Dawley rats were used in group 3 and 4 experiments (see supplemental data). Groups 1 and 2 were used to directly test the hypothesis that brain-wide glymphatic transport of the small molecular weight (MW) paramagnetic contrast agent, gadopentetic acid (Gd-DTPA, MW 938Da), would be superior with dexmedetomidine + low dose isoflurane (DEXM-I) when compared to isoflurane anesthesia. Groups 3 and 4 tested the effects of the two anesthetics regimens on arterial blood gas values of the spontaneously breathing rats measured during MRI, which we assumed would be similar between groups. Finally, and outside the MRI, Groups 5 and 6 were used to test the hypothesis that spindles would be present in the EEG of DEXM-I anesthetized rats compared to isoflurane, indicating different arousal patterns with the two drugs.

MRI experiments (Groups 1 and 2)

All MRI acquisitions were performed on a 9.4T/30 MR instrument interfaced to a Bruker Advance console controlled by Paravision 6.0 software (Bruker Bio Spin, Billerica, MA, USA). Rats were scanned in the supine position using a custom-built animal cradle system; and small earplugs with external gauze pads were accommodated onto the rat's ears to minimize the noise from the scanner. A 2-cm planar surface radio-frequency coil (Bruker) with a built-in pre-amplifier was used as a receiver and an 86-mm diameter volume coil (Bruker) was used as a transmitter.

Anesthesia and surgery for animals undergoing MRI—Group1 and 2 rats underwent implantation of an intrathecal catheter into the cisterna magna (CM) as previously described[14,21]. Following surgery, rats were prepared for MRI and the anesthesia regimen adjusted according to Table 1. For Group 1 rats, isoflurane anesthesia was maintained at 1.5–2.2 % delivered in an 1:1 O_2:air mixture via a nose cone. Exhaled gas from the rats was actively vacuumed away from the nose cone via a build-in vacuum line. For Group 2 rats, 0.015 mg/kg of dexmedetomidine was administered i.p; and followed by a continuous infusion of 0.015–0.020 mg/kg/hr delivered via a subcutaneous catheter. Low

dose isoflurane (0.4–0.8% isoflurane) was used as supplementary anesthesia for Group 2 rats to enhance motor relaxation during the MRI scanning procedure; this anesthesia routine is referred to as 'DEXM-I' in the manuscript. Physiological parameters, including respiratory rate, oxygen saturation, body temperature and heart rate were continuously monitored using an MRI compatible monitoring system (SA Instruments, Stony Brook, NY, USA). Body temperature was kept within a range of 36.5°C~37.5°C using a heated waterbed.

The MRI imaging experiments included 1) pre-contrast T1 mapping for quantitative assessment of gray matter (GM), white matter (WM) and CSF; 2) glymphatic transport characterization using contrast enhanced MRI and 3) MR angiography.

T1 mapping—In a subset of groups 1 and 2 animals, variable flip angle spoiled gradient echo method was implemented to quantify corresponding 3D longitudinal relaxation (T1) maps, which were used for volumetric tissue compartment analyses. Following acquisition of scout images, 3D T1 mapping was performed with the following parameters: TR/TE=15ms/4ms scanning time=4 min. dummy=10, matrix=128×128×128 reconstructed at 0.24×0.24×0.26mm. A set of six flip angles (2°, 5°, 10°, 15°, 20°, 30°) were acquired for T1 maps. The spatial inhomogeneity profile of the RF transmit was acquired using a double angle method[22] as a correction factor for the T1 mapping procedure. Rapid acquisition with relaxation enhancement (RARE) sequence was implemented for B1 mapping of the RF transmit using the following parameters: TR = 10000 ms, TE = 22 ms, Average = 1, RARE factor =4, number of slices =50, in plane resolution = 0.24 mm/pixel, slice-thickness =0.4 mm, slice gap =0.2 mm Flip angles=70° and 140°.

Glymphatic transport MRI—Spoiled gradient echo FLASH 3D images were acquired (TR= 15 ms, TE = 4.1 ms, NEX=1) every 4 minutes. Images were interpolated from 256×128×128 to 256×256×256, yielding a nominal spatial resolution of $0.12\times0.12\times0.13mm^3$. The first three images were taken as baseline images; and Gd-DTPA contrast infusion was started at the beginning of the fourth image. A 1:40 dilution (Gd-DTPA:H_20) was infused at a rate of 1.7μl/min for a total volume of 20 μl. FLASH 3D images were acquired continuously for at least 160 minutes, totaling ~40 frames for each study.

MR angiogram—A 2D time of flight MR angiography (MRA) sequences (TR=12ms TE=2.7ms NEX=4, flip angle = 80°) was taken at the end of the study with a spatial image resolution of $0.12\times0.12\times0.20mm^3$ (256×256×105). Translation and orientation of the 2D MRA were adjusted so that both MRA and FLASH3D images were spatially co-registered.

MRI data analysis

Calculation of 3D T1 maps—3D T1 mapping was performed by linearization of the spoiled gradient echo signal in canonical form, which was then solved voxel-wise by an unweighted linear least square fit algorithm[23]. For calculating T1, the RF inhomogeneity correction factor was applied onto the flip angles to correct for nominal flip angles with actual flip angles[24–26].

T1 map spatial normalization and tissue segmentation—Individual T1 maps were segmented into GM, WM and CSF probability maps using an unified segmentation algorithm in SPM12 (http://www.fil.ion.ucl.ac.uk/spm/)[27] using the *in vivo* rat tissue probability maps[28] as spatially resolved tissue priors. Segmented GM and WM tissue probability maps in native space were then thresholded and summed for calculating total volumes in each compartment.

Analysis of glymphatic transport from contrast enhanced MRI dynamic images—Contrast-enhanced MRI images were processed as previously described[14,21]. Briefly, all images were exported in DICOM and converted into nifti file format to correct for head motion, intensity normalization across the time series, and spatial smoothing. After spatial smoothing, % signal changes from the baseline, were calculated in each voxel as described previously[14,21]. From each of the parametric dynamic MRI images 'Time-Signal-Curves' (TSCs) of Gd-DTPA induced signal changes were extracted using PMOD software (PMOD Technologies Ltd, Zürich, Switzerland, version 3.5) from regions of interest using the baseline MRI as anatomical template. A whole brain parenchymal mask was created for each of the rats' anatomical T1 template by excluding CSF spaces; and the TSCs extracted. TSCs from other regions of interest were extracted from the dynamic T1-weighted images, including the hippocampus and olfactory tubercle. To calculate whole brain Gd-DTPA uptake (representing glymphatic transport) the area-under-curve from of the TSCs (0–180 min) from the whole brain were extracted from the dynamic MRI images from each rat using PMOD software as previously described[21]. From the hippocampal TSCs, time-to-peak, peak magnitude and clearance rates were estimated by linearly fitting the descending trend[29]. Volumetric rendering of Gd-DTPA distribution at various time after CSF administration were enabled using Amira software (FEI, Thermo Fisher Scientific, OR, USA, Version 6.2).

Analysis of MR angiograms (MRA)—The MRAs were reformatted to match the spatial resolution of the 3D FLASH images acquired for visualizing Gd-DTPA glymphatic transport. The MRA analysis was performed similar to that outlined by Li et al.[30]; by implementing the 'auto skeleton' pipeline in Amira software (FEI, Thermo Fisher Scientific, OR, USA, Version 6.2). The MRA image was displayed using maximum intensity projection (MIP); to measure vessel lumen diameter, radial projections perpendicular to the vessel of interest were obtained and the mean diameter along the vessel segment calculated.

Measurement of physiological parameters and blood gases (Groups 3 and 4)

In a separate series of rats (Groups 3 and 4, Supplemental data), we measured physiological parameters, and blood gases receiving either isoflurane or DEXM-I similar to Groups 1 and 2. Rats were initially anesthetized with isoflurane; an arterial catheter was inserted into the femoral artery; and CM catheter sham operation was performed. The skin wounds were closed. The rats were randomly assigned to receive either isoflurane or DEXM-I; and the anesthetic regimens and physiological monitoring was carried out as for Groups 1 and 2. The rats were placed in the 9.4T instrument and MRI scanning was started. Arterial blood gases were acquired twice over 1 hr. The spinal catheter was not perfused with contrast for these experiments (for more details see supplementary data).

EEG measurements during isoflurane and DEXM-I (Groups 5 and 6)

EMG and EEG recording electrodes were prepared as described previously[31]. Briefly, six-channel, custom-made EEG/EMG recording electrodes were prepared by soldering small (<0.75″) segments of insulated 0.008″ silver wire into gold-pin connectors. These electrodes were then combined into a six-channel EEG electrode holder and secured using dental cement. The EEG and EMG recording wires were inserted over the surface of the skull (4 electrodes) and the neck musculature (2 electrodes). For Group 5 rats undergoing EEG recording inhaled with isoflurane, anesthesia was induced with 2–3 % isoflurane in 100% O_2 until the righting reflex was lost and maintained with 1.5–1.8% isoflurane delivered in 1:1 O2: Air mixture via a nose cone. The respiratory rate was maintained between 55–65 bpm by adjusting the isoflurane concentration. For Group 6, rats were first induced with 2–3 % isoflurane in 100% O_2 until loss of the righting reflex; subsequently a 0.015 mg/kg bolus of dexmedetomidine was administered i.p. (repeated 2–4 times if respiratory rate >40 bpm) followed by a continuous infusion of (0.015–0.020 mg/kg/hour) delivered via a subcutaneous catheter placed in the flank area. Low dose isoflurane (0.4–0.8% isoflurane) was used as supplementary anesthesia. The respiratory rate was maintained between ~40 bpm by adjusting the isoflurane concentration. Respiratory rate and temperature were monitored every 10 minutes for 1.5–2 hours. Body temperature was kept within a range of 36.5°C~37.5°C using a heating pad. The rats were in prone position during anesthesia and EEG recordings. EEG recordings were collected using an XLTEK, 32-channel EEG system. Electrodes were referenced to one skull electrode and saved using XLTEK; data were analyzed using customized Matlab scripts to determine percent prevalence (Delta: 1–4 Hz, Theta: 4–8 Hz, Alpha: 8–13 Hz, Beta: 13–32 Hz) and power spectrum.

Statistical analyses

All statistical analyses was performed using XLSTAT Software (Version 2016.5, Addinsoft, Paris France). Sample size for MRI based glymphatic studies (Groups 1 and 2) were based on previous experience[14,21]. Whole brain Gd-DTPA uptake as measured by area-under-curve of the TSCs over 180 min (AUC_{180}), were compared between the two groups using a 2-tailed t test for independent groups and a p-value < 0.05 was considered significant. All continuous variables, heart rate (HR), respiratory rate (RR) and mean blood pressure (see supplemental data) were tested to determine whether they met conditions of normality using Shapiro-Wilk's test. The differential effects of the two anesthesia regimens on heart rate (HR) and respiratory rate (RR) were analyzed by first calculating the mean of these parameters for each rat over 180 min time. Subsequently, the coefficient of variation (CV) of the HR and RR were calculated for each rat over the 180 min of experimental recording. Mann-Whitney, two-tailed test was used to compare the mean HR, RR and mean CVs between the groups. The vessel analysis performed from the MR angiograms were performed blindly. To evaluate group differences (DEXM-I versus isoflurane) between parameters including 1) parameters extracted from the hippocampal TSC (time-to-peak, peak magnitude and clearance rates); 2) vessel diameter, 3) tissue compartments (CSF, WM, GM) and 4) blood gas values, the Student's t test was used if normality was met, and the

Mann-Whitney, two-tailed test was performed if normality was unmet. All data are presented as mean ± SD.

Results

Glymphatic transport of Gd-DTPA during isoflurane anesthesia in comparison to DEXM-I

Kinetic analysis of glymphatic transport has shown that not all brain regions display the same kinetic contrast profiles. Thus for a given experimental time period (2–3 hrs) some brain regions such as the hippocampus show clear uptake and loss while other regions are characterized by slower uptake and little or no loss[14,21]. We first assessed and compared whole brain glymphatic transport from Groups 1 and 2. During the first 40 min (from the time of Gd-DTPA delivery into CSF), whole brain Gd-DTPA uptake was similar between the two anesthetics. However at ~60 min whole brain Gd-DTPA uptake increased with DEXM-I anesthesia compared to isoflurane; and the T1-signal peaked at ~19% and ~12% with DEXM-I and isoflurane, respectively (see Fig. 1A for time-signal curves (TSC)). The quantitative analysis of the total brain uptake of Gd-DTPA as measured by AUC_{180} (representing glymphatic transport over a 180 min CSF circulation period) demonstrated that rats anesthetized with DEXM-I had 32% higher uptake than rats anesthetized with isoflurane (AUC_{180} (brain) DEXM-I (N=8): 2490 ± 446 %*min vs AUC_{180} (brain) isoflurane (N=8): 1697 ± 431 %*min, $p<0.003$). The spatial distribution pattern of whole brain uptake is shown as a volume rendered color-coded map in a DEXM-I anesthetized rat (Fig. 1B) and an isoflurane anesthetized rat (Fig 1C) 2 hrs after start of contrast infusion; and shows more overall tissue penetration of Gd-DTPA in DEXM-I compared to isoflurane.

Fig. 2A shows average scatter plots of hippocampal TSC from rats anesthetized with DEXM-I in comparison to rats anesthetized with pure isoflurane. The hippocampal TSC data can be divided into three time period based on the kinetics: t_1 = 0–12.3 min presents the period of delay from the time of CSF contrast infusion into the CM until the contrast reaches the hippocampus region; t_2 = 12.3–61.5 min presents the period of glymphatic contrast transport where influx is greater than clearance; and t_3 = 61.5–160 min present the period where glymphatic contrast clearance is dominating. In the hippocampus region, the time-to-peak was similar between the two groups: (DEXM-I (N=8) 73.2 ± 8.7 min vs. isoflurane (N=8) 63.0 ± 12.6 min, p-value = 0.079). From the linear regression of t3 where clearance of contrast dominated we extracted peak magnitude and clearance rates (k_{cl}) from each rat of the two groups. The peak magnitude of contrast in DEXM-I anesthetized rats was significantly greater compared to isoflurane anesthetized rats (31.0 ± 9.8% vs 12.6 ± 4.1%, p=0.0017). In addition, the calculated clearance rate was also superior in DEXM-I anesthetized rats compared to isoflurane: (0.12 ± 0.05 %/min vs 0.03 ± 0.02%/min, p=0.0011). The linear regression parameters of the average hippocampal clearance profiles from the two groups are shown in Fig. 2B.

Physiological and cerebral vascular status with the two anesthetics

One explanation for the enhanced glymphatic transport with DEXM-I compared to isoflurane could be related to potential different actions on the cerebral vasculature. Dexmedetomidine has vasoconstrictive properties[32] while isoflurane exert intrinsic

vasodilation[33] and these differences may affect glymphatic transport. The two anesthetics' differential effect on the cerebral vasculature and glymphatic transport is best evaluated if arterial blood pressure and respiratory status is maintained at the same level. During the MRI experiments, vital signs were recorded continuously while the rat underwent scanning. Statistical analysis revealed no differences in the RRs between the two anesthesia groups (RR (DEXM-I) = 52 ± 8 breath per min (BPM) vs RR (isoflurane) = 55 ± 5 BPM, p=0.37) and the RR coefficient of variability for the two groups was also similar (Fig. 3). In contrast, the mean HR for rats anesthetized with DEXM-I was lower than for isoflurane (HR (DEXM-I) = 286 ± 18 beats per min vs HR (isoflurane) = 342 ± 24 beats per min, $p<0.005$), however, heart rate variability (CV) did not differ between groups. To further evaluate physiological profiles, we performed blood gas measurements in separate groups of rats exposed to the same two anesthetic regimes over 1 hr during MRI scanning. These experiments confirmed similar blood gas values between the two anesthetics (supplemental data, Table 1S).

We next explored quantitative differences in the cross-sectional large vessel diameter between the two groups based on the 2D time-of-flight MR angiograms (MRA). We measured the radial projections of four vessels, which are straightforward to locate anatomically including the superior sagittal sinus (SSS), straight sinus (SS), external jugular vein (EJV) and internal carotid artery (ICA). Figs. 4A, B shows typical 3D rendered MRAs displaying the major vascular landmarks including the vessel segments of interest highlighted in red. Isoflurane produced greater vasodilation in the SS when compared to DEXM-I (compare Fig. 4C with Fig. 4D). In contrast, no differences in average vessel diameter were seen in the other 3 vessels measured (Figs. 4E, F; Table 2).

GM, WM and CSF volume effects of the two anesthetics

Reduced uptake of Gd-DTPA with isoflurane when compared to DEXM-I suggests that the CSF had restricted access to the brain's glymphatic pathway. We used the quantitative T1 maps to extract the volumes of the GM, WM and CSF tissue compartments. Table 3 shows the quantitative data for total brain volume (TBV), GM, WM and CSF. As expected there was no difference in total brain volume between the two groups (TBV, isoflurane = 1611 ± 117 mm^3 vs TTV, DEXM-I = 1695 ± 49 mm^3). The CSF compartment was significantly decreased with isoflurane compared to DEXM-I (CSF (isoflurane) = 54 ± 8 mm^3 vs CSF (DEXM-I) = 85 ± 7 mm^3, $p < 0.01$), supporting the statement that less CSF gains access to the brain with isoflurane.

If CSF is not entering into the glymphatic system with isoflurane to the same extent as with DEXM-I, CSF must be diverted to other sites for reabsorption. We characterized efflux of Gd-DTPA at the olfactory portion of the nasal cavity which is known to participate in CSF efflux[34]. The limited MRI field-of-view did not allow us to capture more distant areas (e.g. naso- and maxilla-turbinates); but the endoturbinates could be assessed. The location of the olfactory portion of the nasal cavity, which represents the innermost zone containing the endoturbinates is shown in sagittal (Fig. 5A) and cross sectional (Fig. 5B) T1-weighed MRI; note the typical spiral lamella at the level of the endoturbinates. As can be seen in Fig 5C, Gd-DTPA efflux in a rat anesthetized with isoflurane (50 min after CSF administration)

displays a distribution pattern similar to the outline of the endoturbinates, suggesting that it ends up in nasal submucosa similar to what has been reported in the literature[34]. Fig. 5D shows the average TSCs from the nasal cavity from rats anesthetized with isoflurane versus DEXM-I. Both the average peak signal amplitude (51.5% vs 39.0%, $p<0.05$), and the time-to-peak (isoflurane: 54.3 ± 4.7 min vs DEXM-I: 72.4 ± 5.6 min, $p < 0.001$) is significantly higher for isoflurane compared to DEXM-I. Together, these results suggest that for the same time period, more CSF carrying Gd-DTPA enters into the endoturbinates with isoflurane compared to DEXM-I.

EEG changes with isoflurane versus DEXM-I

In separate groups of rats (Groups 5 and 6, Table 1) EEG profiles were recorded under the two different anesthetic regimens. Fig. 6 shows an example of an EEG spectrogram (2D, density spectral array, Fig. 6A); and an unprocessed EEG trace from a rat anesthetized with isoflurane (Fig. 6B); and the corresponding EEG display in a rat anesthetized with DEXM-I (Figs. 6C, D). In the rat anesthetized with isoflurane, the 2D spectrogram representing a 7 min segment (Fig. 6A), shows that during the first 2 min the EEG is dominated by slow delta (1–4Hz) and alpha (9–12Hz) oscillations; followed by burst suppression. Burst suppression is described as "a state of unconsciousness and profound brain inactivation"[18] and the raw, unprocessed EEG will often display this as alternating periods of isoelectricity and electrical activity as shown in Fig. 6B. In the rats anesthetized with isoflurane, episodes of burst suppression was observed when the respiratory rate was ~50 BPM (isoflurane ~1.5%). In the rats anesthetized with DEXM-I (isoflurane ~0.6%), spindle oscillations (9–15 Hz) could be observed; and examples are shown in Figs 6C and D. In the DEXM-I anesthetized rats, the spindle frequency varied; and most often the EEG was dominated by slow delta oscillations. Spindle oscillations were never observed in the rats anesthetized with isoflurane.

Discussion

In this study, we compared the effects of DEXM-I with pure isoflurane anesthesia on the brain's glymphatic transport efficiency to address the question of whether drugs that produce 'unconsciousness' all enhance glymphatic transport to the same extent. We hypothesized that unconsciousness produced in rodents receiving supplementary dexmedetomidine, a potent selective α2 agonist, given its blocking effect on central norepinephrine release[17,35] would enhance glymphatic transport greater than those receiving pure isoflurane. This hypothesis was based on previous data by Xie et al., showing that glymphatic transport (when compared to wakefulness) was dramatically increased by (a) xylazine/ketamine anesthesia, (b) deep wave sleep and by (c) alpha antagonists administered directly onto the cortex[13]. Using the MRI method previous developed[21] for quantifying glymphatic transport, we showed that glymphatic transport of the rodent brain was indeed significantly increased with DEXM-I anesthesia compared to isoflurane.

When stimulated, presynaptic α2 receptors inhibits norepinephrine release in the brain including the locus coeruleus (LC)[17], which has the highest density of α2 receptors in the brain[36]. LC neurons project to the basal forebrain, preoptic area (POA), hypothalamus, thalamus and cortex[18,37]. The effect of norepinephrine blockade on the POA, in particular,

has wide ranging 'upstream' effects involving several neurotransmitters and neural networks, leading to decreased arousal, sleep-like states or deep sedation[18]. In contrast, isoflurane (a halogenated inhalational anesthetic) exerts its effects by acting on a wide variety of voltage- and ligand-gated channels including $GABA_A$, glycine, nicotinic acetylcholine receptors, NMDA and K channels [19,38], which are located throughout the brain and spinal cord. The effects of isoflurane on LC neurons and NE are not as clear cut as those of dexmedetomidine. Though isoflurane has been shown to depress LC activity (this effect is most pronounced during the night cycle where LC neurons are most active)[39]; rats anesthetized with 2% isoflurane show increases in POA norepinephrine [40]. Given the divergent effects of dexmedetomidine and isoflurane on norepinephrine, we expected enhanced glymphatic transport with DEXM-I anesthesia compared with isoflurane only anesthesia. Xie et al. administered alpha antagonists directly onto cortex of mice and observed the same increase in glymphatic transport as in deep sleep in comparison to wakefulness. Due to the experimental design which necessitated the low dose isoflurane with dexmedetomidine our study cannot strictly distinguish between effects of dexmedetomidine, effects of low dose isoflurane, or effects of the combination DEXM-I when compared to high dose Isoflurane. However, the enhanced glymphatic transport with DEXM-I compared to isoflurane is likely attributed to the potent effect of dexmedetomidine on central norepinephrine release as the systemic sympatholytic effects were evident by a lower heart rate in rats receiving supplementary dexmedetomidine. In humans, intravenous DEXM infusion also reduces systemic sympathetic tone with baroreflex sensitivity preserved[41].

The low-dose isoflurane and dexmedetomidine anesthetic regimen used in our study, was previously shown to maintain blood-oxygen-level dependent (BOLD) fMRI-neuronal activity coupling; and was introduced specifically for rodent functional MRI brain imaging studies to demonstrate the presence of the default mode network (DMN)[42]. The demonstration of a preserved DMN with DEXM-I is strongly suggestive of a lighter state of sedation/anesthesia since the DMN is known to be inhibited with increasing levels of anesthesia[43]. Based on this information, it is to be expected that although the rats in our study were all 'unconscious' during measurement of glymphatic transport, the rats anesthetized with pure isoflurane were in a deeper state of anesthesia compared to the rats anesthetized with DEXM-I. To further investigate anesthetic depth of the two anesthetic regimens, we recorded EEG in a separate series of rats (who did not undergo MRI). In the rats receiving DEXM-I, the EEG was characterized by slow-wave oscillations and spindles, while the EEG with isoflurane only showed burst patterns intermingled with slow delta and alpha oscillations. These data confirm that that anesthesia with pure isoflurane produces a deeper state of anesthesia as evidenced by burst suppression compared to DEXM-I. In human subjects the EEG during dexmedetomidine sedation is characterized by slow-delta oscillations with spindles, which resemble stage II non-rapid eye movement sleep[18]. With increasing dexmedetomidine dosing and depth of sedation (unresponsive to verbal commands), the slow-delta oscillations dominate as in stage III sleep[18]. With isoflurane administered at 1 MAC concentration or higher, the EEG is characterized by, slow delta, alpha and theta oscillations; and burst pattern. In summary, the two anesthetic drug regimens used in our experiments both produced unconsciousness (loss of righting reflex) but they had

different effects on glymphatic transport, emphasizing that the underlying molecular signature of the drug producing unconsciousness is more important than anesthetic depth per se.

Xie et al., showed that when mice were asleep or anesthetized with ketamine/xylazine the ISF space volume increased by 40–60% in cortex when compared to wakefulness, presumably reflecting cell volume shrinkage[13]. Accordingly, assuming that dexmedetomidine reduces central norepinephrine, the reason for enhanced glymphatic transport would suggest that ISF space volume also increases more with DEXM-I when compared to isoflurane, thereby allowing more CSF to enter the brain to exchange with ISF. In support of this statement, the quantitative analysis of tissue compartments based on T1 maps revealed that the CSF compartment was significantly larger (~2%) in DEXM-I anesthetized rats compared to isoflurane only. This result suggests that more CSF enters the glymphatic pathway in the rats anesthetized with DEXM-I thereby enhancing convective solute exchange and transport. It is important to point out, that we only measured CSF volume and not CSF production. Other studies have shown that Isoflurane anesthesia does not appear to affect CSF production[44], but may affect reabsorption. The possibility that isoflurane may affect CSF reabsorption patterns is supported by evidence of enhanced egress of Gd-DTPA via the olfactory nerves in isoflurane anesthetized rats when compared to DEXM-I (Fig. 5)

The respiratory rate of the rats in the two anesthesia groups were similar during the MRI experiments and it is unlikely therefore that hypercarbia, secondary vasodilation and increased ICP are explanatory factors for the observed differences in the glymphatic transport. This statement is supported by data from a separate group of rats demonstrating similar arterial blood gases with the two anesthetics. Future experiments quantifying ICP would be required to rule out this possibility. However, inhalational anesthetics including isoflurane are known to have intrinsic vasodilatory effects. Indeed, the MR angiograms did suggest that certain vascular beds such as the straight sinus was more dilated with isoflurane compared to DEXM-I (Fig. 4). Since the SS is situated near the pineal recess, which is a large CSF reservoir in the rat brain, extreme SS dilatation with isoflurane anesthesia might also explain the observed reduced influx of CSF. Further improvement in quantitative MRA analysis and supplementary quantitative measurement of cerebral blood volume (CBV) and cerebral blood flow (CBF) will be needed to more fully address the impact of divergent vascular beds on glymphatic transport with the two anesthetics. However, previous rodent studies have shown that isoflurane anesthesia delivered at 1.7% results in ~50% increase in CBF and ~10% increase in CBV in comparison to propofol[45]. It is also known that sedation with low dose dexmedetomidine decreases CBF up to 30% in healthy volunteers[32] and it has been suggested that this effect is in part due to stimulation of α_{2B}-receptors by dexmedetomidine producing vasoconstriction. However, we did not observe vasoconstriction at the level of the ICA in the DEXM-I anesthetized rats when compared to isoflurane, which could be due to the low-dose of isoflurane used and/or limitation in our techniques.

Limitations of the study

The MRI-based platform for quantifying glymphatic transport in the rodent brain has been validated using optical imaging and fluorescently-tagged dyes administered into CSF[1,14,21]. Thus both peri-arterial influx, and parenchymal uptake of the MR contrast agent has been shown to mimic peri-arterial and parenchymal transport of small-molecular weight fluorescently tagged dyes[21]. From these studies a quantitative measure of 'glymphatic transport' and clearance have been derived. However, it has to be pointed out that brain parenchymal 'clearance' of the extracellular, metabolically inert solute Gd-DTPA is a net effect of redistribution and elimination; and thus it is possible that the enhanced clearance observed in DEXM-I anesthetized rats compared to isoflurane reflects faster redistribution rather than true clearance. Further investigations with other solutes and quantitative tools will help determine these parameters more accurately.

Potential clinical implications

The brain's glymphatic pathway has received tremendous research attention because of its role in removal of metabolic wastes, including soluble Aβ and tau[1,2], and the therapeutic potential of manipulating this pathway for preventing or slowing down Alzheimer's disease (AD)[46]. In addition, the notion that sleep enhances Aβ clearance via the glymphatic pathway and the fact that chronic sleep disorders are associated with a higher risk for development of AD[47] suggests that potentially simple preventive clinical measures such as facilitating better overall quality sleep might help reduce the risk of AD. Although not yet demonstrated, there are data in support of a human glymphatic pathway including: 1) circadian variation in the CSF concentration of aβ and tau[48], 2) larger Aβ burden in older adults who are reporting poorer sleep quality[49], and 3) a significant loss of AQP4 expression in post mortem human brains afflicted with AD[10]. Thus assuming that a glymphatic pathway exists in the human brain, several implications for clinical care undoubtedly will emerge in the near future.

In this study we show that compared to isoflurane, DEXM-I enhances glymphatic transport and increases CSF volume in the rodent brain. This is important because dexmedetomidine is known to reduce other anesthetic agent requirements, and is used as an adjunct in many clinical settings for sedation and/or anesthesia. Thus, it is possible that it would be advantageous to use dexmedetomidine with the goal of improving postoperative cognitive performance by improving 'brain waste removal' during anesthesia and/or sedation procedures. In support of this conjecture, increasing clinical evidence is emerging that dexmedetomidine may prevent delirium in elderly patients after surgery[50,51], while a recent study showed that a prophylactic low-dose infusion of dexmedetomidine in patients admitted to the ICU after non-cardiac surgery decreased the incidence of delirium in the first 7 days[52].

Supplementary Material

Refer to Web version on PubMed Central for supplementary material.

Acknowledgments

The authors greatly acknowledge the assistance of Mei Yu, BS, Department of Anesthesiology, Stony Brook Medicine, Stony Brook NY, USA for technical help with the animal MRI experiments.

Funding Statement: NIH R01AG048769 and RF1 AG053991, NIDA-IRP, Leducq Foundation

References

1. Iliff JJ, Wang M, Liao Y, Plogg BA, Peng W, Gundersen GA, Benveniste H, Vates GE, Deane R, Goldman SA, Nagelhus EA, Nedergaard M. A paravascular pathway facilitates CSF flow through the brain parenchyma and the clearance of interstitial solutes, including amyloid beta. Sci Transl Med. 2012; 4:147ra111.
2. Iliff JJ, Chen MJ, Plog BA, Zeppenfeld DM, Soltero M, Yang L, Singh I, Deane R, Nedergaard M. Impairment of glymphatic pathway function promotes tau pathology after traumatic brain injury. J Neurosci. 2014; 34:16180–93. [PubMed: 25471560]
3. Lundgaard I, Lu ML, Yang E, Peng W, Mestre H, Hitomi E, Deane R, Nedergaard M. Glymphatic clearance controls state-dependent changes in brain lactate concentration. J Cereb Blood Flow Metab. 2016
4. Peng W, Achariyar TM, Li B, Liao Y, Mestre H, Hitomi E, Regan S, Kasper T, Peng S, Ding F, Benveniste H, Nedergaard M, Deane R. Suppression of glymphatic fluid transport in a mouse model of Alzheimer's disease. Neurobiol Dis. 2016; 93:215–25. [PubMed: 27234656]
5. Bechter K, Hof PR, Benveniste H. On the flow dynamics of cerebrospinal fluid. Neurology, Psychiatry and Brain Research. 2015; 21:96–103.
6. Cserr HF, Cooper DN, Suri PK, Patlak CS. Efflux of radiolabeled polyethylene glycols and albumin from rat brain. Am J Physiol. 1981; 240:F319–28. [PubMed: 7223889]
7. Louveau A, Smirnov I, Keyes TJ, Eccles JD, Rouhani SJ, Peske JD, Derecki NC, Castle D, Mandell JW, Lee KS, Harris TH, Kipnis J. Structural and functional features of central nervous system lymphatic vessels. Nature. 2015; 523:337–41. [PubMed: 26030524]
8. Zakharov A, Papaiconomou C, Djenic J, Midha R, Johnston M. Lymphatic cerebrospinal fluid absorption pathways in neonatal sheep revealed by subarachnoid injection of Microfil. Neuropathol Appl Neurobiol. 2003; 29:563–73. [PubMed: 14636163]
9. Kress BT, Iliff JJ, Xia M, Wang M, Wei HS, Zeppenfeld D, Xie L, Kang H, Xu Q, Liew JA, Plog BA, Ding F, Deane R, Nedergaard M. Impairment of paravascular clearance pathways in the aging brain. Ann Neurol. 2014; 76:845–61. [PubMed: 25204284]
10. Zeppenfeld DM, Simon M, Haswell JD, D'Abreo D, Murchison C, Quinn JF, Grafe MR, Woltjer RL, Kaye J, Iliff JJ. Association of Perivascular Localization of Aquaporin-4 With Cognition and Alzheimer Disease in Aging Brains. JAMA Neurol. 2016
11. Sakka L, Coll G, Chazal J. Anatomy and physiology of cerebrospinal fluid. Eur Ann Otorhinolaryngol Head Neck Dis. 2011; 128:309–16. [PubMed: 22100360]
12. Iliff JJ, Wang M, Zeppenfeld DM, Venkataraman A, Plog BA, Liao Y, Deane R, Nedergaard M. Cerebral arterial pulsation drives paravascular CSF-interstitial fluid exchange in the murine brain. J Neurosci. 2013; 33:18190–9. [PubMed: 24227727]
13. Xie L, Kang H, Xu Q, Chen MJ, Liao Y, Thiyagarajan M, O'Donnell J, Christensen DJ, Nicholson C, Iliff JJ, Takano T, Deane R, Nedergaard M. Sleep drives metabolite clearance from the adult brain. Science. 2013; 342:373–7. [PubMed: 24136970]
14. Lee H, Xie L, Yu M, Kang H, Feng T, Deane R, Logan J, Nedergaard M, Benveniste H. The Effect of Body Posture on Brain Glymphatic Transport. J Neurosci. 2015; 35:11034–44. [PubMed: 26245965]
15. Ding F, O'Donnell J, Xu Q, Kang N, Goldman N, Nedergaard M. Changes in the composition of brain interstitial ions control the sleep-wake cycle. Science. 2016; 352:550–5. [PubMed: 27126038]
16. Keating GM, Hoy SM, Lyseng-Williamson KA. Dexmedetomidine: a guide to its use for sedation in the US. Clin Drug Investig. 2012; 32:561–7.
17. Jorm CM, Stamford JA. Actions of the hypnotic anaesthetic, dexmedetomidine, on noradrenaline release and cell firing in rat locus coeruleus slices. Br J Anaesth. 1993; 71:447–9. [PubMed: 8104450]

18. Purdon PL, Sampson A, Pavone KJ, Brown EN. Clinical Electroencephalography for Anesthesiologists: Part I: Background and Basic Signatures. Anesthesiology. 2015; 123:937–60. [PubMed: 26275092]
19. Mashour GA, Forman SA, Campagna JA. Mechanisms of general anesthesia: from molecules to mind. Best Pract Res Clin Anaesthesiol. 2005; 19:349–64. [PubMed: 16013686]
20. Kushikata T, Hirota K, Kotani N, Yoshida H, Kudo M, Matsuki A. Isoflurane increases norepinephrine release in the rat preoptic area and the posterior hypothalamus in vivo and in vitro: Relevance to thermoregulation during anesthesia. Neuroscience. 2005; 131:79–86. [PubMed: 15680693]
21. Iliff JJ, Lee H, Yu M, Feng T, Logan J, Nedergaard M, Benveniste H. Brain-wide pathway for waste clearance captured by contrast-enhanced MRI. J Clin Invest. 2013; 123:1299–309. [PubMed: 23434588]
22. Stollberger R, Wach P. Imaging of the active B1 field in vivo. Magn Reson Med. 1996; 35:246–51. [PubMed: 8622590]
23. Frahm J. Rapid FLASH NMR imaging. Naturwissenschaften. 1987; 74:415–22. [PubMed: 3683588]
24. Chang LC, Koay CG, Basser PJ, Pierpaoli C. Linear least-squares method for unbiased estimation of T1 from SPGR signals. Magn Reson Med. 2008; 60:496–501. [PubMed: 18666108]
25. Cheng HL, Wright GA. Rapid high-resolution T(1) mapping by variable flip angles: accurate and precise measurements in the presence of radiofrequency field inhomogeneity. Magn Reson Med. 2006; 55:566–74. [PubMed: 16450365]
26. Deoni SC, Peters TM, Rutt BK. Determination of optimal angles for variable nutation proton magnetic spin-lattice, T1, and spin-spin, T2, relaxation times measurement. Magn Reson Med. 2004; 51:194–9. [PubMed: 14705061]
27. Ashburner J, Friston KJ. Unified segmentation. Neuroimage. 2005; 26:839–51. [PubMed: 15955494]
28. Valdes-Hernandez PA, Sumiyoshi A, Nonaka H, Haga R, Aubert-Vasquez E, Ogawa T, Iturria-Medina Y, Riera JJ, Kawashima R. An in vivo MRI Template Set for Morphometry, Tissue Segmentation, and fMRI Localization in Rats. Front Neuroinform. 2011; 5:26. [PubMed: 22275894]
29. Lee H, Mortensen K, Sanggaard S, Koch P, Brunner H, Quistorff B, Nedergaard M, Benveniste H. Quantitative Gd-DOTA uptake from cerebrospinal fluid into rat brain using 3D VFA-SPGR at 9.4T. Magn Reson Med. 2017
30. Li Y, Shen Q, Huang S, Li W, Muir ER, Long JA, Duong TQ. Cerebral angiography, blood flow and vascular reactivity in progressive hypertension. Neuroimage. 2015; 111:329–37. [PubMed: 25731987]
31. Veasey SC, Valladares O, Fenik P, Kapfhamer D, Sanford L, Benington J, Bucan M. An automated system for recording and analysis of sleep in mice. Sleep. 2000; 23:1025–40. [PubMed: 11145318]
32. Prielipp RC, Wall MH, Tobin JR, Groban L, Cannon MA, Fahey FH, Gage HD, Stump DA, James RL, Bennett J, Butterworth J. Dexmedetomidine-induced sedation in volunteers decreases regional and global cerebral blood flow. Anesth Analg. 2002; 95:1052–9. table of contents. [PubMed: 12351293]
33. Matta BF, Heath KJ, Tipping K, Summors AC. Direct cerebral vasodilatory effects of sevoflurane and isoflurane. Anesthesiology. 1999; 91:677–80. [PubMed: 10485778]
34. Johnston M, Zakharov A, Koh L, Armstrong D. Subarachnoid injection of Microfil reveals connections between cerebrospinal fluid and nasal lymphatics in the non-human primate. Neuropathol Appl Neurobiol. 2005; 31:632–40. [PubMed: 16281912]
35. Callado LF, Stamford JA. Alpha2A- but not alpha2B/C-adrenoceptors modulate noradrenaline release in rat locus coeruleus: voltammetric data. Eur J Pharmacol. 1999; 366:35–9. [PubMed: 10064149]
36. Zilles K, Qu M, Schleicher A. Regional distribution and heterogeneity of alpha-adrenoceptors in the rat and human central nervous system. J Hirnforsch. 1993; 34:123–32. [PubMed: 7901270]
37. Akeju O, Loggia ML, Catana C, Pavone KJ, Vazquez R, Rhee J, Contreras Ramirez V, Chonde DB, Izquierdo-Garcia D, Arabasz G, Hsu S, Habeeb K, Hooker JM, Napadow V, Brown EN, Purdon

PL. Disruption of thalamic functional connectivity is a neural correlate of dexmedetomidine-induced unconsciousness. Elife. 2014; 3:e04499. [PubMed: 25432022]

38. Pal D, Silverstein BH, Lee H, Mashour GA. Neural Correlates of Wakefulness, Sleep, and General Anesthesia: An Experimental Study in Rat. Anesthesiology. 2016; 125:929–942. [PubMed: 27617688]
39. Gompf H, Chen J, Sun Y, Yanagisawa M, Aston-Jones G, Kelz MB. Halothane-induced hypnosis is not accompanied by inactivation of orexinergic output in rodents. Anesthesiology. 2009; 111:1001–9. [PubMed: 19809293]
40. Anzawa N, Kushikata T, Ohkawa H, Yoshida H, Kubota T, Matsuki A. Increased noradrenaline release from rat preoptic area during and after sevoflurane and isoflurane anesthesia. Can J Anaesth. 2001; 48:462–5. [PubMed: 11394514]
41. Hogue CW Jr, Talke P, Stein PK, Richardson C, Domitrovich PP, Sessler DI. Autonomic nervous system responses during sedative infusions of dexmedetomidine. Anesthesiology. 2002; 97:592–8. [PubMed: 12218525]
42. Lu H, Zou Q, Gu H, Raichle ME, Stein EA, Yang Y. Rat brains also have a default mode network. Proc Natl Acad Sci U S A. 2012; 109:3979–84. [PubMed: 22355129]
43. Guldenmund P, Demertzi A, Boveroux P, Boly M, Vanhaudenhuyse A, Bruno MA, Gosseries O, Noirhomme Q, Brichant JF, Bonhomme V, Laureys S, Soddu A. Thalamus, brainstem and salience network connectivity changes during propofol-induced sedation and unconsciousness. Brain Connect. 2013; 3:273–85. [PubMed: 23547875]
44. Abas M, Vanderpyl J, Le Prou T, Kydd R, Emery B, Foliaki SA. Psychiatric hospitalization: reasons for admission and alternatives to admission in South Auckland, New Zealand. Aust N Z J Psychiatry. 2003; 37:620–5. [PubMed: 14511092]
45. Todd MM, Weeks J. Comparative effects of propofol, pentobarbital, and isoflurane on cerebral blood flow and blood volume. J Neurosurg Anesthesiol. 1996; 8:296–303. [PubMed: 8884627]
46. Nedergaard M. Neuroscience. Garbage truck of the brain Science. 2013; 340:1529–30. [PubMed: 23812703]
47. Ooms S, Overeem S, Besse K, Rikkert MO, Verbeek M, Claassen JA. Effect of 1 night of total sleep deprivation on cerebrospinal fluid beta-amyloid 42 in healthy middle-aged men: a randomized clinical trial. JAMA Neurol. 2014; 71:971–7. [PubMed: 24887018]
48. Roh JH, Jiang H, Finn MB, Stewart FR, Mahan TE, Cirrito JR, Heda A, Snider BJ, Li M, Yanagisawa M, de Lecea L, Holtzman DM. Potential role of orexin and sleep modulation in the pathogenesis of Alzheimer's disease. J Exp Med. 2014; 211:2487–96. [PubMed: 25422493]
49. Spira AP, Gamaldo AA, An Y, Wu MN, Simonsick EM, Bilgel M, Zhou Y, Wong DF, Ferrucci L, Resnick SM. Self-reported sleep and beta-amyloid deposition in community-dwelling older adults. JAMA Neurol. 2013; 70:1537–43. [PubMed: 24145859]
50. Brown EN, Purdon PL, Van Dort CJ. General anesthesia and altered states of arousal: a systems neuroscience analysis. Annu Rev Neurosci. 2011; 34:601–28. [PubMed: 21513454]
51. Jansson CC, Pohjanoksa K, Lang J, Wurster S, Savola JM, Scheinin M. Alpha2-adrenoceptor agonists stimulate high-affinity GTPase activity in a receptor subtype-selective manner. Eur J Pharmacol. 1999; 374:137–46. [PubMed: 10422650]
52. Vemparala S, Domene C, Klein ML. Computational studies on the interactions of inhalational anesthetics with proteins. Acc Chem Res. 2010; 43:103–10. [PubMed: 19788306]

Summary Statement

Rats anesthetized with dexmedetomidine and low dose isoflurane had increased glymphatic transport compared to rats anesthetized with isoflurane only. We propose that anesthetics affect the brain's glymphatic transport to a different extent dependent on their mechanism of action.

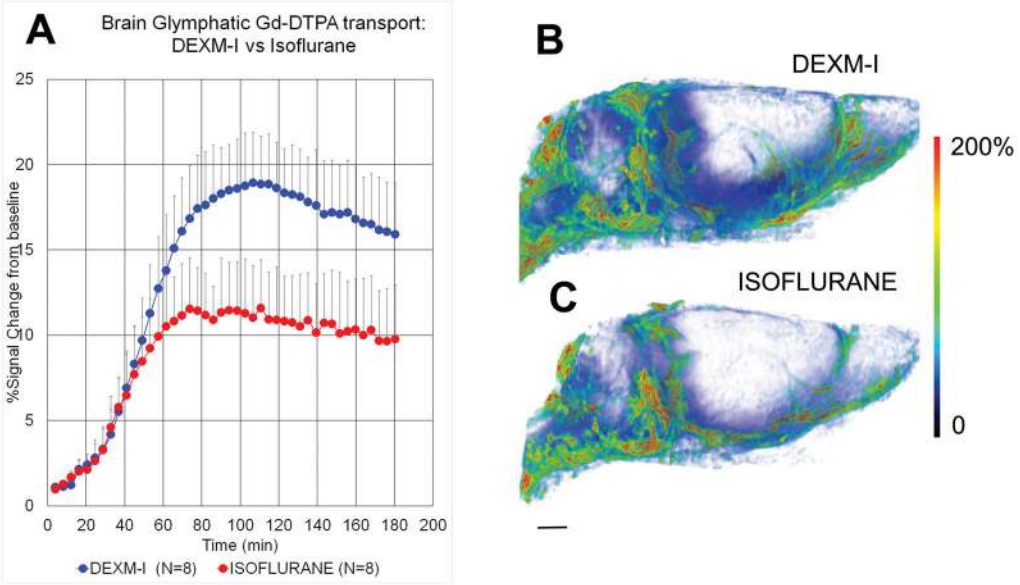

Fig. 1. Dexmedetomidine and low-dose isoflurane (DEXM-I) enhances glymphatic transport of Gd-DTPA in comparison to isoflurane

A: Average time signal curves (TSC) of Gd-DTPA induced signal changes from whole brain of rats anesthetized with DEXM-I (blue, filled circles) and isoflurane (red, filled circles). The TSCs were extracted from the dynamic contrast-enhanced T1-weighted MRIs and represent glymphatic transport of brain parenchyma (excluding cerebrospinal fluid compartment). There is overall more whole brain uptake (as measured by % signal change from baseline) of Gd-DTPA in the DEXM-I anesthetized rats when compared to isoflurane (see result section for quantitative details). The data are expressed as mean ± SD. **B and C:** 3D volume rendered color-coded maps of Gd-DTPA induced signal changes 2hrs after administration of contrast into the CSF from a rat anesthetized with DEXM-I (B) and isoflurane (C). The red and blue colors represent high and low contrast uptake, respectively. Over the first 2 hrs of contrast circulation more contrast had penetrated the brain in the DEXM-I rat (B) when compared to isoflurane (C). Scale bar: 3 mm.

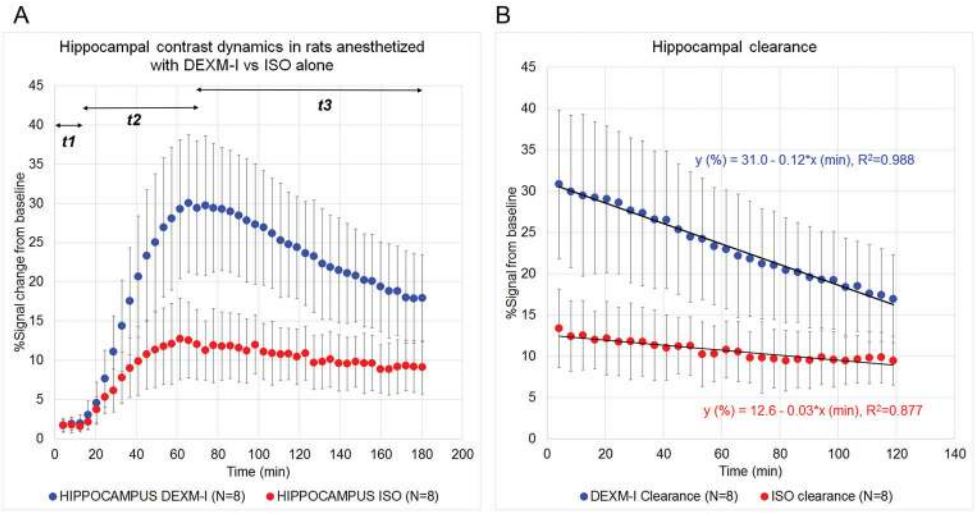

Fig. 2. Glymphatic transport in the hippocampus of rats anesthetized with dexmedetomidine + isoflurane (DEXM=I) and isoflurane

A shows average scatter plots of hippocampal time signal curves (TSC) from rats anesthetized with DEXM-I (blue) in comparison to rats anesthetized with pure isoflurane (red). The hippocampal TSC data can be divided into three time period based on the kinetics: t_1 = 0–12.3 min presents the period of delay from the time of contrast infusion into the cerebrospinal fluid until the contrast reaches the hippocampus region; t_2 = 12.3–61.5 min presents the period of glymphatic contrast transport where influx is greater than clearance; and t_3 = 61.5–160 min present the period where glymphatic contrast clearance is dominating. The linear regression parameters of the average hippocampal clearance profiles from the two groups (DEXM-I, blue; and isoflurane, red) are shown in **B**. Data are presented at mean ± SD. ISO = isoflurane.

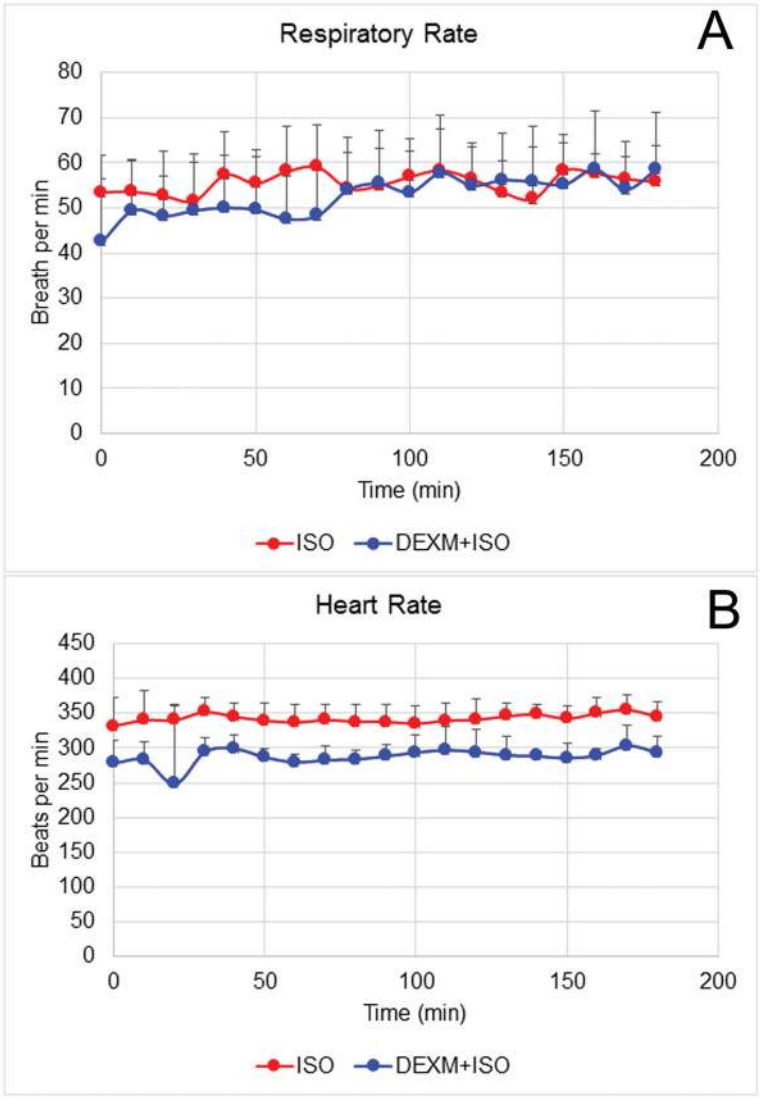

Fig. 3. Physiological parameters during MRI scans

Respiratory rate and heart rate were recorded non-invasively during measurement of glymphatic transport with MRI. The respiratory rate for isoflurane and DEXM-I anesthesia groups were similar over the 2–3 hr experimental period (**A**). The heart rate was significantly lower in DEXM-I rats compared to isoflurane anesthetized rats (**B**). The data are expressed as mean ± SD. ISO = isoflurane.

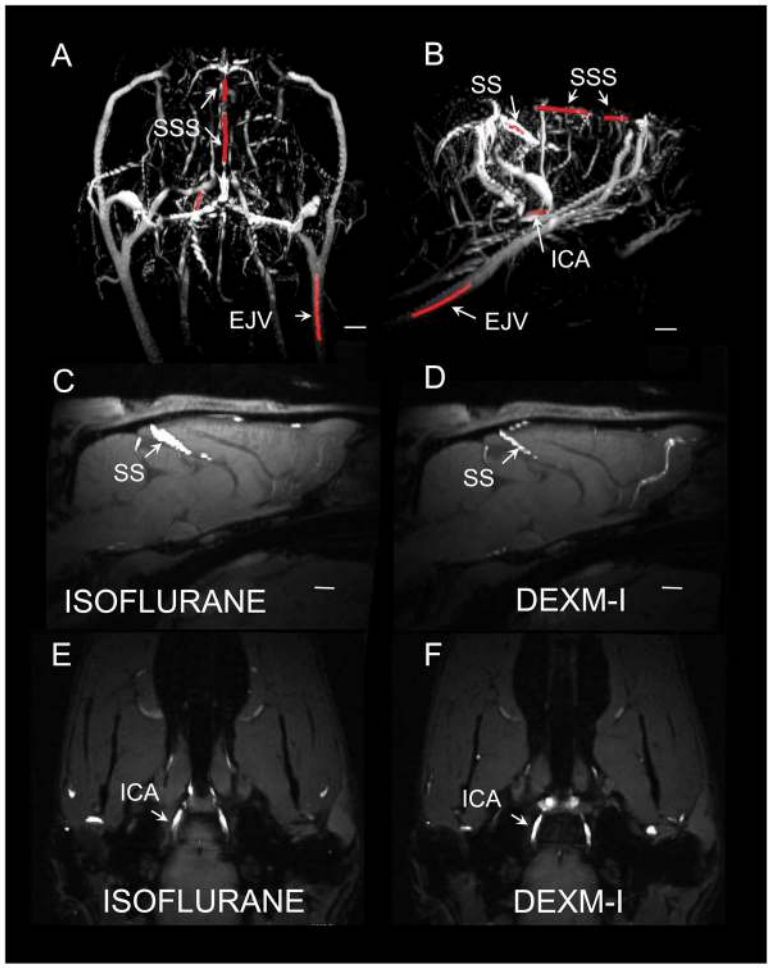

Fig. 4. MR angiograms from rat anesthetized with isoflurane versus dexmedetomidine + isoflurane (DEXM-I)

A, B shows typical 3D volume rendered MR angiograms (maximum intensity projections) displaying the major vascular landmarks including the vessel segments of interest highlighted in red. SSS=superior sagittal sinus; SS=straight sinus, ICA=internal carotid artery; EJV=external jugular vein. **C–F** show 2D MR angiograms overlaid on the corresponding T1 weighted MRIs. Isoflurane produced greater vasodilation in the SS when compared to DEXM-I (compare **C** with **3D**). In contrast, no differences in average vessel diameter were observed at the level of the ICA (compare **Figs. E, F).** Scale bar: 2 mm.

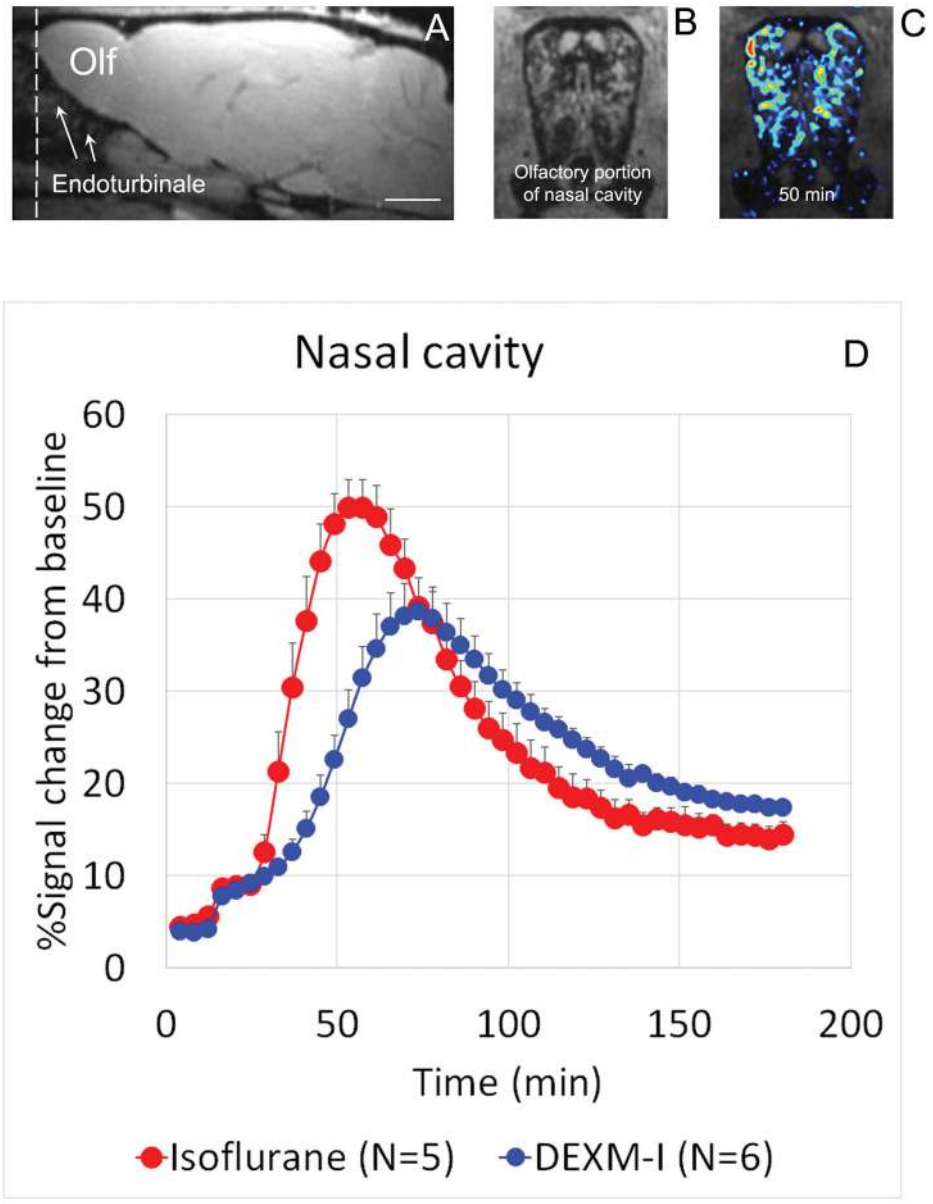

Fig. 5. MR contrast (Gd-DTPA) efflux via the olfactory nerves

A: Sagittal T1-weighted MRI at the level of the olfactory bulb and endoturbinates. The field of view includes the olfactory portion of the nasal cavity (Olf=olfactory bulb). Scale bar: 3 mm. The dashed line indicates the cross-sectional area for the nasal cavity shown in **B** (anatomy displayed) and **C** (color coded MR contrast map representing Gd-DTOA after 50 min of cerebrospinal fluid circulation overlaid on the anatomical map). As can be observed in **C**, the distribution pattern of contrast follows the surface curvature of the endoturbinates. **D:** Average time signal curves (TSCs) acquired from the endoturbinates of rats anesthetized with isoflurane (red) vs dexmedetomidine + isoflurane (DEXM-I, Blue). Quantitative analysis show that the time-to-peak and peak amplitude of Gd-DTPA induced signal changes are significantly higher in isoflurane compared to DEXM-I anesthetized rats. The data are

presented as mean ± SD. The data were extracted from the contrast-enhanced MRIs via an anatomical mask of the olfactory portion of the nasal cavity.

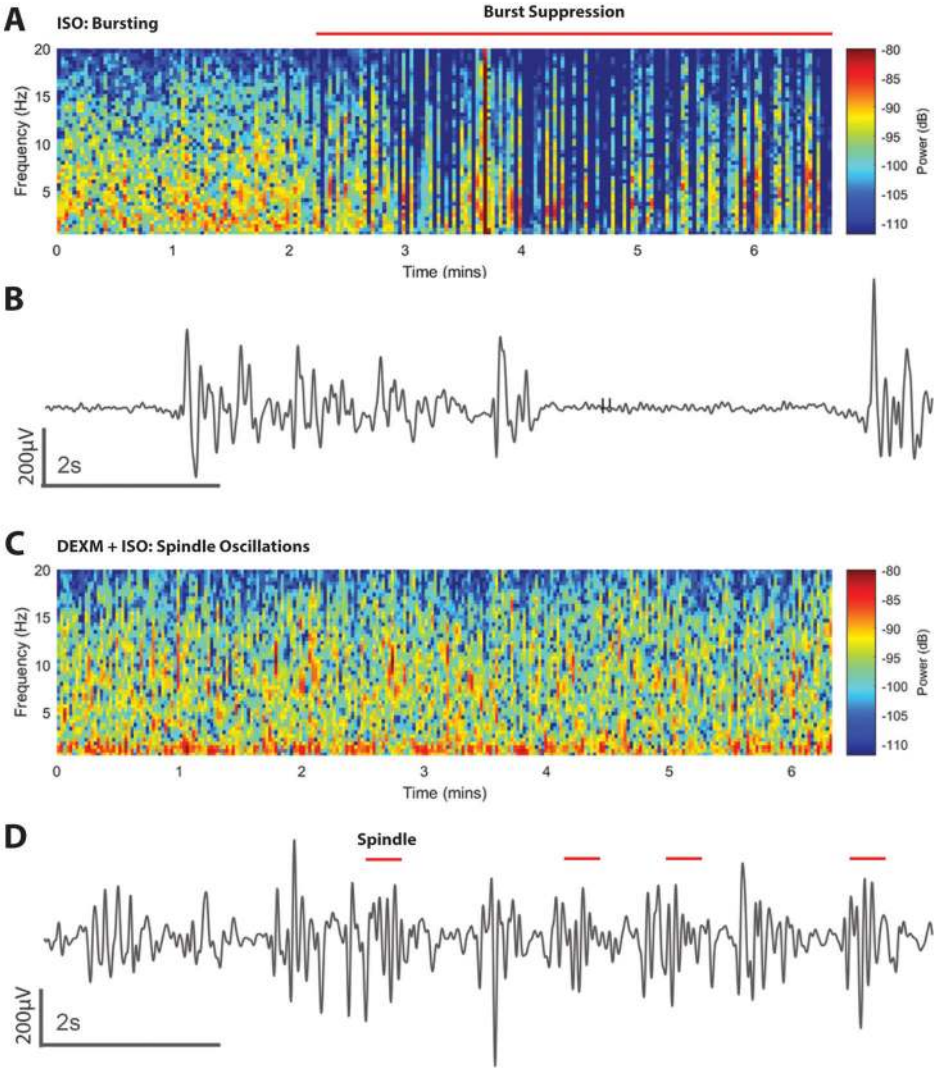

Fig. 6. Spectrograms and time domain electroencephalogram (EEG) signatures of isoflurane and dexmedetomidine + isoflurane (DEXM-I)

A. 2D Spectrogram of EEG from a rat receiving isoflurane. Burst suppression in the spectrogram is shows as periods of blue (isoelectric activity) interspersed with periods of red-yellow (delta and theta oscillations). The horizontal red line shows the principal period of burst suppression. **B**. Ten-second electroencephalogram trace from A showing burst events (intermittent high amplitude activity) and suppression events (isoelectric activity). **C**. 2D EEG spectrogram from a rat receiving DEXM-I. The spectrogram shows spindles (intermittent red period 9–15Hz) and slow-delta oscillations. **D.** Ten-second electroencephalogram trace from the period in C emphasizing spindles (red lines). ISO = isoflurane.

Table 1

Experimental Groups and Experiments

Groups	Anesthesia	Experiment	MRI	Arterial line	EEG
1 (N=8)	Isoflurane	Characterizing glymphatic transport of Gd-DTPA	Yes	No	No
2 (N=8)	DEXM-I		Yes	No	No
3* (N=4)	Isoflurane	Characterizing physiological parameters	Yes	Yes	No
4* (N=4)	DEXM-I		Yes	Yes	No
5 (N=4)	Isoflurane	Characterizing EEG	No	No	Yes
6 (N=4)	DEXM-I		No	No	Yes

*Female Sprague Dawley rats were used for the additional studies (see supplemental data for more information). DEXM-I = Dexmedetomidine + low dose isoflurane.

Table 2

Vessel diameter differences between the two groups.

Average vessel diameter (μm)	Isoflurane (N=8)	DEXM-I (N=6)	p-value
SSS	159 ± 49	139 ± 47	0.192
SS	307 ± 73	127 ± 26	0.002
EJV	567 ± 13	448 ± 98	0.107
ICA	245 ± 59	245 ± 38	1.000

Data are presented as mean ± SD.

*Only 6 of the 8 rats in the DEXM-I anesthesia group (Group 2) underwent MRA analysis. DEXM-I = Dexmedetomidine + low dose isoflurane.

Table 3

Total brain volume and tissue compartments between the two groups

	Total Brain volume (mm^3)	Grey matter volume mm^3	White matter volume mm^3	CSF volume mm^3
Isoflurane (N=4)	1611 ± 112	924 ± 113	633 ± 41	54 ± 8
DEXM-I (N=4)	1695 ± 49	931 ± 50	681 ± 25	84 ± 7
p-value	0.210	0.602	0.076	0.009

Data are presented as mean ± SD. DEXM-I = Dexmedetomidine + Isoflurane.